

ANALYSIS OF THE INFLUENCE OF MAGNETIC INDUCTION RAMP PROFILE ON AXIAL FORCE AND FRICTION TORQUE GENERATED BY MR FLUID

Wojciech HORAK*, Marcin SZCZĘCH*

*AGH University of Science and Technology Faculty of Mechanical Engineering and Robotics,
Department of Machine Design and Technology, al. Mickiewicza 30, 30-059 Cracow, Poland

horak@agh.edu.pl, szczech@agh.edu.pl

received 21 July 2019, revised 10 July 2019, accepted 15 July 2019

Abstract: The unique properties of magnetic fluids result from their ability to undergo reversible, almost immediate, changes in their rheological properties under the influence of magnetic fields as well as the possibility to position them by magnetic field forces. It is also possible to control the direction and flow rate of such fluids. These properties provide an efficient way to develop new types of controllable machines and devices, such as brakes, clutches and bearings. The objective of the study was to examine the axial force and torque friction of a magnetorheological (MR) fluid working in the shear flow mode (parallel plate system) subjected to different magnetic induction ramp profiles. The rotation speed and working gap height were also taken into account. Determining the response of the tested system to magnetic induction change in different working conditions was of particular interest.

Key words: MR Fluid, Axial Force, Torque, Control, Experiments, Magnetic Field Ramp

1. INTRODUCTION

Magnetorheological (MR) fluids are smart materials with controllable rheological characteristics that may be modified by external magnetic fields. These materials are suspensions of particles made of ferromagnetic material immersed in a carrier fluid that does not exhibit magnetic properties. MR fluids consist of particles with a size of up to a few micrometres, unlike ferrofluids (FFs) that are produced based on the particles with a diameter of several nanometres (Raj et al., 1995; Rosenweig, 1985; Vekas, 2008). The magnetic particles are usually covered with a surface-active compound in order to prevent the aggregation and sedimentation of the suspension. The properties of the fluid may be different because of the changes in the microstructure of the suspension occurring in the magnetic field (Odenbach et al., 2007). In the macroscopic scale, the magnetic field affects the stress state in a fluid in both the tangential (Lopez-Lopez et al., 2010; Odenbach et al., 2007; See and Tanner, 2003) and normal directions (Guo and Gong, 2012; Horak et al., 2017a, b). The range of change in rheological properties is a function of several factors, in particular, volume fraction of the magnetic particles in the fluid, magnetic properties of the particle material, surfactant type, carrier fluid type, particle size and shape. The behavior of MR fluids also depends on deformation conditions such as deformation rate (Horak et al., 2017b), flow direction [pressure (Kubik et al., 2017), shear (Guo and Gong, 2012; Jang et al., 2011; See and Tanner, 2003) or squeeze flow mode (Hegger and Maas, 2016)] and magnetic field distribution.

MR fluids are used in various technical applications, such as vibration dampers (Ajay Kumar et al., 2016; Bajkowski, 2012; Jaszczkowski and Sapiński, 2017), brakes and clutches (Guldbake and Hesselbach, 2006), valves (Lopez-Lopez et al., 2010), bearings (Horak et al., 2017b) and precision polishing (Wang et al., 2016).

The parallel plate system used in the tests occurs in both measuring devices, for example, in the case of testing the rheological properties of magnetic fluids, as well as controllable devices, such as brakes or thrust bearings (Laun et al., 2008).

In the case of rheological tests, flow curves or the viscous and elastic modulus are determined under the influence of the magnetic field. But in contrast to this type of research, this publication describes the laboratory tests of the axial force and torque friction generated by selected MR fluids in this system. Different rotational speed and gap heights are considered. The phenomena occurring inside the MR fluid structure during the magnetic induction change are complicated and depend on many parameters (Chen et al., 2013). The purpose of the work was to describe the transient states of the particle structure change in the fluid observed during measurements in the case of increasing and decreasing ramp profile of magnetic field induction. The test results show the problems of using this type of fluid in controllable systems.

2. EXPERIMENTAL SETUP

The research experiments were performed on a test stand for the examination of magnetic fluids in shear and squeeze flow modes, described in detail in Horak et al. (2017c). The scheme of the device is presented in Figure 1a. On the support frame, there is an axial drive consisting of a linear servo motor (1) on which a rotary servo motor (2) is mounted.

An essential part of the measurement system is the torque and axial force transducer (3) on which the measuring plate is mounted. The examined sample is placed in the test cell (4). The scheme of the test cell is shown in Figure 1b. The magnetic fluid (6) is placed in the measuring gap formed between the flat rotary plate (5) and the core of the electromagnet (8). The value of magnetic induction is controlled by the current in the coil of the

electromagnet (9). A magnetic circuit is closed by the lower and upper parts of the test cell (7). Some elements (7 and 8) are made of ferromagnetic material. The rotary plate is made of a material with paramagnetic properties. The diameter of electromagnet core is $d_r = 45$ mm, and that of rotary plate is 60 mm. The height of magnetic gap is $z = 9$ mm. The height of the measuring gap h is adjustable by a linear servomotor with an accuracy of $\pm 1 \mu\text{m}$.

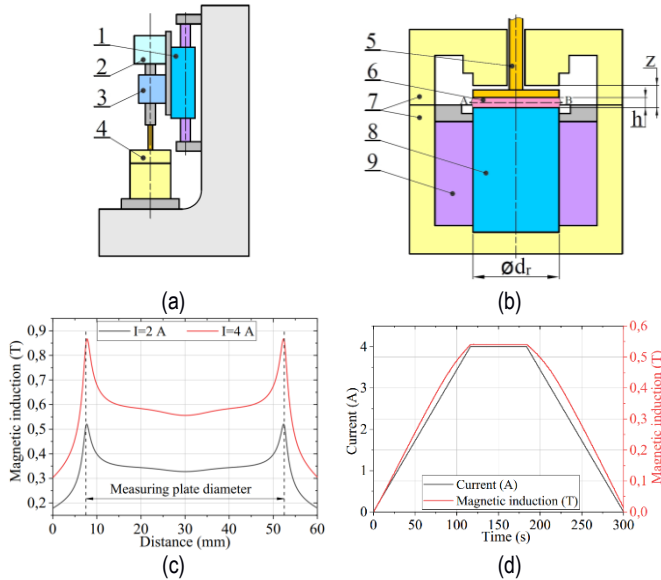


Fig. 1. (a) General view of the test stand, (b) scheme of the test stand, (c) scheme of the test cell and (d) distribution of the magnetic induction in the gap

Figure 1c shows the magnetic induction distribution in the measuring gap (measurement between Points A and B; see Fig. 1b). The magnetic induction is not a constant value on the plate diameter. On the edge of the core there is a local increase in the value. This provides the self-sealing effect [10] and the magnetic fluid is held in the region of the measuring gap. In turn, in the electromagnet core axis region, there are local decreases in the magnetic induction because of the opening present in the upper part of the test cell.

The tests were carried out for three measuring gap heights $h = 0.25, 0.5$ and 1 mm; the volume of the MR fluids was, respectively, $v = 0.4, 0.8$ and 1.6 ml. Each measurement was performed at the rotational speeds of $n = 0, 1, 10, 50$ and 100 min^{-1} . The trapezoidal current curve in the electromagnet coil was within the range $I = 0\text{--}4$ A, which corresponded to the magnetic induction $B = 0\text{--}540$ mT. The coil current curve can be divided into three stages: increase during 115 s, next stabilisation for 70 s and then decrease for the next 115 s. The slope of current change is 0.34 A/min . The current change and the corresponding magnetic field induction are shown in Figure 1d. Magnetic induction measurement was performed in the middle of the measuring plate diameter. In the electromagnet core and in the lower and upper parts of the test cell, there are orifices through which the coolant fluid flows. This provides temperature stabilisation of the cell. The tests were carried out under thermal stabilisation conditions at 20°C .

The examined fluid was hydrocarbon-based MR fluid (type: MRF-122EG) produced by LORD Corporation. It is known from the product card that the magnetic particle volume fraction is

estimated as 22%, and the viscosity at 40°C in the absence of the magnetic field is $42 \text{ mPa}\cdot\text{s}$. The saturation magnetisation is 360 kA/m . The fluid choice resulted from the relatively small particle volume fraction and the high saturation magnetisation. This fluid also has a wide range of applications, such as shock dampers and brakes.

Magnetic circuit elements have ferromagnetic properties and are characterised by residual magnetisation that is present when an external magnetic field is removed. Therefore, before every measurement, a demagnetising procedure was carried out. Demagnetisation was accomplished by supplying the electromagnet coil with a sinus function decaying in time (see Horak et al., 2017c). This ensured the repeatability conditions under which the research was conducted.

3. RESULTS AND DISCUSSION

Figure 2 shows the results of axial force and torque measurement obtained at various rotational speeds and gap heights. For all cases, the axial force value (Fig. 2 a–c) observed in time differs significantly from the shape of the magnetic induction ramp. The smallest force values are achieved for the gap $h = 0.25$ mm and when the plate is not rotating.

Moreover, in the case of non-rotating plates, for different gaps, high force maintains for some time as a relatively constant value despite lowering magnetic induction. A similar phenomenon has been observed in Salwiński and Horak (2011). This behavior indicates that the normal force in MR fluids is the result not only of the magnetostatic pressure (Rosenweig, 1985), but even after magnetic field decay, the force can be maintained (in the absence of other extortions). This may be associated with the formation of lattice structures of ferromagnetic particles in the MR fluid, and especially the interaction of friction forces between particles (Hegger and Mass, 2016; Li and Zang, 2008). It can be seen that, during the first stage of the experiment, the axial force response is delayed compared to the current changes, with this phenomenon particularly visible in the absence of rotational speed.

Over in the time interval (0–25 s), the force for a certain time has a local upward trend, which temporarily undergoes a downward or stabilising trend and, for the case shown in Figure 2a, the force for some time even takes a negative value (about -4 N). This is probably due to the fact that, for some time, the particles in the MR fluid move towards the region of the highest magnetic induction (see Fig. 1c).

In an upward trend, the axial force curves for all speeds are similar, whereas the results obtained for the downward magnetic induction ramp show that, for all cases at higher rotational speeds, the axial force has lower values. This is probably associated with faster structure destruction inside the magnetic fluid, see also Gong et al. (2012), Guo and Gong (2012) Lopez-Lopez et al. (2010) and See and Tanner (2003). However, as the presented test results show, the influence of rotational speed on the normal force also depends on the ramp direction of magnetic field change.

During the second experiment stage (constant current), after a certain time, the force stops growing, and in the case of the speeds of $0, 1$ and 10 min^{-1} , a constant value of the force, or even an increase, is observed. At 50 and 100 min^{-1} , in most cases, the force begins to decrease over time or some fluctuations are observed. Assuming the influence of the internal structure of MR

fluid on the value of the axial force, such results indicate that there is a limit rotational speed below which shearing does not decrease or even improve the ability of MR fluid to generate normal force. The state of magnetic particle chain formation can be considered through an analysis of the interplay between magnetic and hydrodynamic interactions, typically expressed using the Mason number (Klingenberg et al., 2007). The presence of sufficiently small

Mason number values (at low rotational speed) encourages the formation of internal MR fluid structures (Shan et al., 2015). In addition, the shear deformation of MR fluid changes the contact conditions among the particles, thus changing the frictional forces (Hegger and Maas, 2016; Li and Zhang, 2008), with such a hypothesis additionally confirming the obtained results.

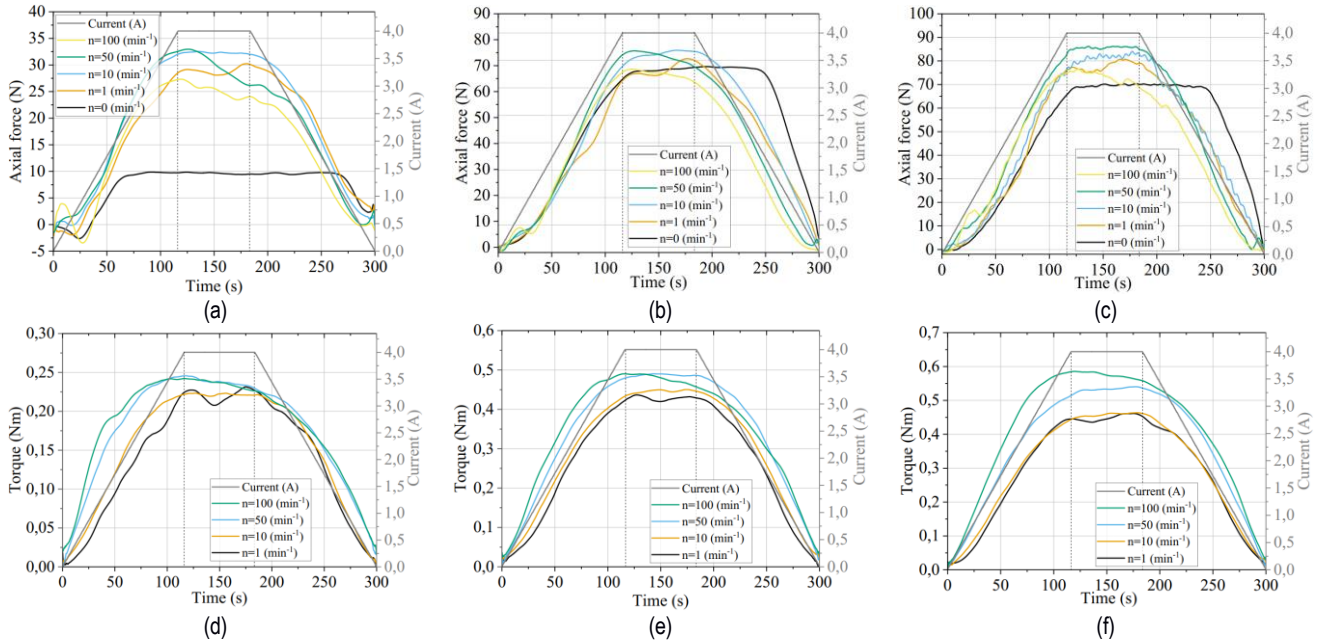


Fig. 2. Axial force measurement: (a) $h = 0.25$ mm, (b) $h = 0.5$ mm and (c) $h = 1$ mm. Torque measurement: (d) $h = 0.25$ mm, (e) $h = 0.5$ mm and (f) $h = 1$ mm

In Figure 3, the axial force slopes during the time of current increasing and decreasing trends were shown. On the basis of the results, it can be concluded that the higher gap and the presence of rotational speed accelerates and facilitates the formation of axial force to a certain extent.

Figure 2d–f shows torque changes over measuring time. The curves, compared to the force response, are more similar in the shape of the applied current change (Fig. 1d). An asymmetry in value is also noticeable when comparing increasing and decreasing trends, which may be related to the magnetic hysteresis of the measuring cell elements. In the stage of constant current, the torque does not stabilise and, in most cases, a slight decrease in torque can be observed.

downward trends (see Fig. 4). Generally, higher slopes are observed for higher measuring gap heights. In the analysed case, there is no noticeable trend determining the impact of rotational speed on this parameter.

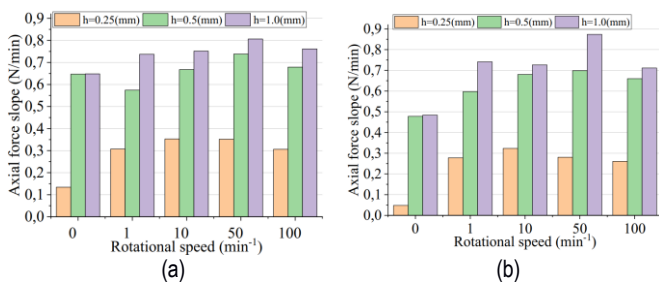


Fig. 3. Axial force slope: (a) current upward trend and (b) current downward trend

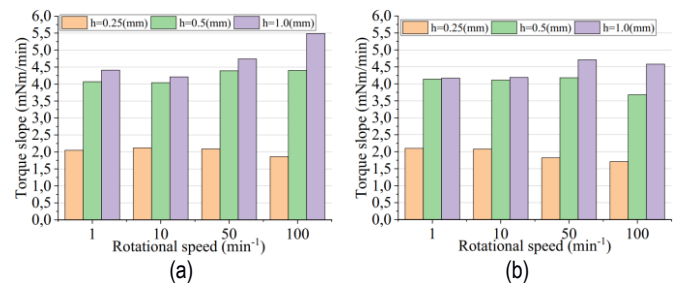


Fig. 4. Torque slope: (a) current upward trend and (b) current downward trend

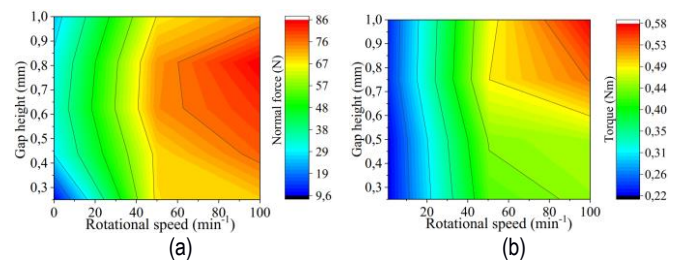


Fig. 5. Contour plots of mean: (a) axial force and (b) torque

In the case of torque measurement, no significant differences are observed in the case of slope value between the upward and

Figure 5 shows contour plots illustrating the influence of the gap height and rotational speed on the axial force and torque. The charts were developed based on the average value measured during the constant current stage, and the graphs are the result of measured data interpolation.

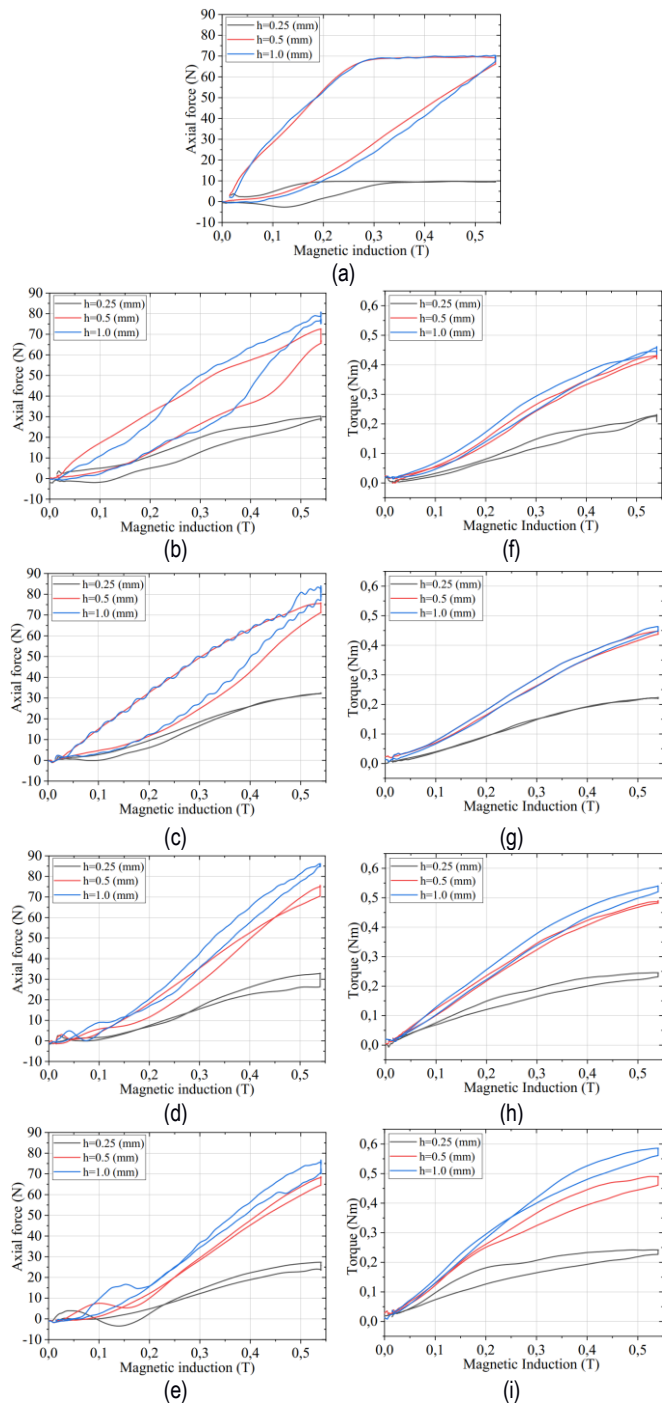


Fig. 6. Axial force versus magnetic induction hysteresis loops: (a) $n = 0$, (b) $n = 1$, (c) $n = 10$, (d) $n = 50$ and (e) $n = 100 \text{ min}^{-1}$ and torque versus magnetic induction hysteresis loops: (f) $n = 1$, (g) $n = 10$, (h) $n = 50$, (i) $n = 100 \text{ min}^{-1}$

As can be seen in Figure 5a, specified rotational speed and gap height values favour obtaining the highest axial force. Relatively small and excessively large gap height lowers the axial force. In the case of torque, higher values are observed for higher rotational speeds as well. Increasing the height of the working gap

leads to higher values of torque (Fig. 5b). In the general case, an increase in torque (shear stress) according to the Bingham model as a result of increased shear rate is expected (Horak et al., 2017b). As can be seen, the obtained results also show the significant influence of the MR fluid volume (layer height). The shear rate for higher rotational speed (100 min^{-1}) and the narrowest gap (0.25 mm) are 4 times higher in relation to the same rotational speed and the widest measuring gap (1 mm), but the measured torque is 2.6 times lower for a narrower gap.

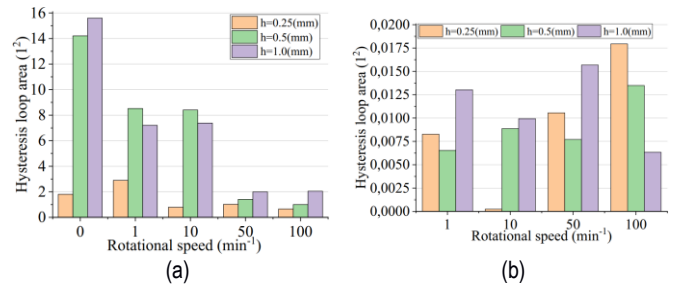


Fig. 7. Hysteresis loop area for (a) axial force and (b) torque

Figure 6 shows measured parameters versus magnetic induction as hysteresis loops. For the axial force when the measuring plate is non-rotating (Fig. 6a), $h = 0.25 \text{ mm}$, the force reaches its maximum value at a relatively low magnetic field induction (about 0.15 T), however, the obtained force values are the lowest. Rotational speed (Fig. 6b–e) improves the ability to generate axial force, moreover, as shown in Figure 7a; for these measurements, the results have been obtained with a smaller hysteresis loop area, which may indicate an improvement in controlling the axial force in the presence of rotation.

In the case of torque curves (Fig. 6f–i), hysteresis loops are smaller (even several times) than those in the case of axial force (compare Fig. 7a to 7b). This observation is consistent with other experimental work (Szczęch and Horak, 2017).

4. CONCLUSIONS

An important aspect of MR fluid application in controllable machines and devices, such as brakes, clutches and bearings, is the ability to change the value of the force and the torque as a result of the magnetic induction variation. The main conclusions from the conducted studies can be formulated as follows:

- The axial force and torque value are significantly dependent on the height of the working gap and the rotational speed.
- Narrow as well as relatively wide gaps adversely affect the fluid ability to generate a normal force. This dependence is particularly noticeable at low rotational speeds.
- Owing to the ability of the MR fluid to generate the highest axial force, it is advantageous to subject the MR fluid to a correspondingly high deformation rate. Excessively high deformation causes a reduction in the axial force.
- The rotational speed may adversely affect the stability in the time of the axial force at certain magnetic field parameters (see Fig. 2a–c).
- Under the same rotational speeds, higher values of torque are observed for higher measuring gap heights.

- The response of the MR fluid in the form of a change in axial force and friction torque has a distinctly different course. A more complex issue is definitely the control of the axial force than the torque.

REFERENCES

1. **Ajay Kumar H. N., Shilpashree D. J., Adarsh M. S., Amith D., Kulkarni S.** (2016), Development of Smart Squeeze Film Dampers for Small Rotors, *Procedia Engineering*, 144, 790-800,
2. **Bajkowski J.M.** (2012), Design, analysis and performance evaluation of the linear, magnetorheological damper, *Acta Mechanica et Automatica*, 6(1), 5-9.
3. **Chen S., Huang J., Shu H., Sun T., Jian K.,** (2013) Analysis and Testing of Chain Characteristics and Rheological Properties for Magnetorheological Fluid, *Advances in Materials Science and Engineering*, 2013, 1-6.
4. **Gong X., Guo, Ch., Xuan Sh., Liu T., Zong L., Peng Ch.** (2012), Oscillatory normal forces of magnetorheological fluids, *Soft Matter*, 8(19), 5256-5261,
5. **Guldbakke J. M., Hesselbach J.** (2006), Development of bearings and a damper based on magnetically controllable fluids, *Journal of Physics*, 18, 2959.
6. **Guo Ch.Y., Gong X.L.** (2012,) Normal forces of magnetorheological fluids under oscillatory shear, *Journal of Magnetism and Magnetic Materials*, 324(6), 1218-1224.
7. **Hegger C. and Maas J.** (2016) Investigation of the squeeze strengthening effect in shear mode, *J. Intell. Mater. Syst. Struct.*, 27 1895–907.
8. **Horak W., Salwiński J., Szczęch M.** (2017a), Analysis of the influence of selected factors on the capacity of thrust sliding bearings lubricated with magnetic fluids, *Tribologia*, 48(4), 33–38.
9. **Horak W., Salwiński J., Szczęch M.** (2017b), Experimental Study on Normal Force in MR Fluids Under Low and High Shear Rates, *Machine Dynamics Research*, 41(1), 89-100.
10. **Horak W., Salwiński J., Szczęch M.** (2017c), Test stand for the examination of magnetic fluids in shear and squeeze flow mode, *Tribologia*, 48(2), 67–75.
11. **Jang K.I., Min B.K., Seok J.** (2011), A behavior model of a magnetorheological fluid in direct shear mode, *Journal of Magnetism and Magnetic Materials*, 323(10), 1324-1329.
12. **Jastrzębski Ł., Sapiński B.** (2017), Experimental Investigation of an Automotive Magnetorheological Shock Absorber, *Acta Mechanica et Automatica*, 11(4), 253-259.
13. **Klingenberg D.J., Ulicny J.C., Golden M.A.** (2007), Mason numbers for magnetorheology, *Journal of Rheology*, 51(5), 883–893;
14. **Kubik M., Macháček O., Strecker Z., Roupec J., Mazúrek I.** (2017), Design and testing of magnetorheological valve with fast force response time and great dynamic force range, *Smart Material and Structure*, 26 047002.
15. **Laun H. M., Schmidt G., Gabriel C., Kieburg C.,** (2008) Reliable plate–plate MRF magnetorheometry based on validated radial magnetic flux density profile simulations, *Rheologica Acta*, 47(9), 1049-1059.
16. **Li W., Zhang X.** (2008), The effect of friction on magnetorheological fluids, *Korea-Aust. Rheol. J.*, 20, 45–50.
17. **López-López M.T., Kuzhir P., Durán J.D.G, Bossis G.** (2010), Normal stresses in a shear flow of magnetorheological suspensions: Viscoelastic versus Maxwell stresses, *Journal of Rheology*, 5(5), 1119-1136
18. **Odenbach S., Pop L.M., Zubarev A.Yu.** (2007), Rheological properties of magnetic fluids and their microstructural background, *GAMM-Mitt*, 1, 195-204.
19. **Raj K., Moskowitz B., Casciari R.** (1995), Advances in ferrofluid technology, *Journal of Magnetism and Magnetic Materials*, 149, 174-180.
20. **Rosensweig R.E.** (1985), *Ferrohydrodynamics*, Cambridge University Press, Cambridge.
21. **Salwiński J., Horak W.** (2011), Measurement of normal force in magnetorheological and ferrofluid lubricated bearings, *Key Engineering Materials*, 490, 25-32.
22. **See H., Tanner R.** (2003), Shear rate dependence of the normal force of a magnetorheological suspension, *Rheologica Acta*, 42(1-2), 166-170.
23. **Shan L., Chen K., Zhou M., Zhang X., Meng Y., Tian Y.** (2015), Shear history effect of magnetorheological fluids, *Smart Materials and Structures*, 24(10), 105030.
24. **Szczęch M., Horak W.** (2017), Numerical simulation and experimental validation of the critical pressure value in ferromagnetic fluid seals, *IEEE Transactions on Magnetics*, 53(7), 1–5.
25. **Vekas L.** (2008), Ferrofluids and Magnetorheological Fluids, *Advances in Science and Technology*, 54, 127-136.
26. **Wang Y., Yin S., Huang H.,** (2016) Polishing characteristics and mechanism in magnetorheological planarization using a permanent magnetic yoke with translational movement, *Precis. Eng.*, 43, 93–104.

This work is financed by AGH University of Science and Technology, Faculty of Mechanical Engineering and Robotics, research program No. 16.16.130.942